Quantitative Evaluation of Fatigue Crack Size Using Eddy Current Pulsed Thermography

Feng Fuzhou[1,2*], *Xu Chao*[2], *Zhu Junzhen*[2,3], *Min Qingxu*[2], *Sun Jiwei*[2]

1. Key Laboratory of Nondestructive Testing of Ministry of Education, Nanchang Aeronautical University, Nanchang 330063, P. R. China
2. Department of Mechanical Engineering, Academy of Armored Force Engineering, Beijing 100072, P. R. China
3. School of Electrical and Electronic Engineering, Newcastle University, Newcastle upon Tyne NE1 7RU, UK

(Received 18 September 2016; revised 2 May 2017; accepted 12 May 2017)

Abstract: A set of metallic specimens containing fatigue cracks with different sizes were tested using eddy current pulsed thermography (ECPT), therefore the relations between heating response of the crack area and the crack length was studied. The numerical and experimental results both showed that the increase of the crack length enhanced the crack heating response under specific test conditions. A particular form of calculated response signal, which is linearly related to the crack length, was introduced to provide a quantitative evaluation of crack length.

Key words: ECPT; fatigue crack; heating response; quantification

CLC number: TN219 **Document code**: A **Article ID**: 1005-1120(2017)03-0247-08

0 Introduction

Eddy current pulsed thermography (ECPT) is an active thermography method which combines pulsed eddy current stimulation and infrared (IR) thermography techniques to provide a fast and high resolution of defect detection[1-2]. ECPT can induce a larger electromagnetic power in the specimen, so that the transient temperature response is more obvious. Besides, the pulsed excitation and response contains a wide range of frequencies, which can provide sufficient information for defect feature extraction in frequency domain[3]. The basic principle of ECPT is electromagnetic law and Joule heating. The excitation module generates a short period of high frequency pulsed current, which is driven to the excitation coil above the conductive material. Then the current in the coil will induce eddy currents inside the specimen, which will be perturbed due to the presence of defects. The eddy current energy is further transformed into Joule heat, causing different temperature distribution. Temperature rise on its surface by pulsed heating and heat conduction is captured by IR camera. An indication of defects can be identified immediately through infrared images and quantitative information of defects[4-5] can be obtained through further analysis. Regarding this technique, many researchers have investigated transient temperature response during and after pulsed heating[6-7]. Ren et al extracted the divergence value of the expansion (or contraction) rate of carbon fiber reinforced polymer (CFRP) material and fluid volume and studied the positive and negative values of the divergence and their relation between composite structures and material state. A Quantitative non-destructive evaluation (QNDE) of impact damage with ECPT from divergence patterns and image areas is derived[8]. He et al extracted two characteristic features from differential phase spectra, blind frequency, and minimum phase, and their monotonic relations with defects' depth under different heating time were compared[9]. Abidin et al has

* Corresponding author, E-mail address: fengfuzhou@tsinghua.org.cn.

How to cite this article: Feng Fuzhou, Xu Chao, Zhu Junzhen, et al. Quantitative evaluation of fatigue crack size using eddy current pulsed thermography[J]. Trans. Nanjing Univ. Aero. Astro., 2017, 34(3): 247-254.
http://dx.doi.org/10.16356/j.1005-1120.2017.03.247

extracted and presented the slope inclination feature of the transient temperature distribution, in order to estimate the angle of slots that is independent from the slot depth and the length inside the sample[10]. At present, the quantitative research on ECPT is mainly aimed at finding specific parameters to evaluate the location and size of defects, but there is little research on the quantitative study of fatigue crack.

In this work, features from temperature distribution of fatigue cracks were extracted to achieve quantitative evaluation of the crack length. Multiphysics simulations were carried out to provide initial results and analysis for defect characterization. Through multiphysics simulations, a relation between features and defect length has been obtained. Then the experimental work verified the numerical results and analysis.

1 Electromagnetic Thermal Coupling Model

Establishment of electromagnetic and thermal coupling model is crucial to accurate analysis of quantitative evaluation. During induction heating, the heating patterns are mainly affected by the excitation frequency, power supply, material conductivity and permeability. The skin depth is an important factor in induction heating, which is directly affected by the excitation frequency and material properties. It is defined as the depth at which the eddy current density is equal to the surface eddy current density $1/e$ (37%)

$$\delta = \frac{1}{\sqrt{\pi \mu \sigma f}} \tag{1}$$

where μ is the material permeability, σ the material conductivity and f the excitation frequency.

The temperature of the conductor increases due to the Joule heat generated by the induced current. Joule heatenergy is denoted as Q, which is proportional to the square of the current density, and the current density is proportional to the electric field strength

$$Q = \frac{1}{\sigma} |J_s|^2 = \frac{1}{\sigma} |\sigma E|^2 \tag{2}$$

where J_s is the induced current density, E the electric field intensity.

Ignoring the effect of thermal convection and thermal radiation, the heat conduction equation of the Joule heat generated in the measured object can be expressed as

$$\rho C_p \frac{\partial T}{\partial t} - \nabla (\sigma_T \nabla) = Q \tag{3}$$

where ρ is the material density, C_p the heat capacity, σ_T the thermal conductivity, and T the temperature.

The assessment of defects is mainly based on the perturbation of the current distribution resulting in different heating patterns, and it can be represented by a basic model, as shown in Fig. 1. The crack is filled with air in the model, and the impedance is approximated as infinity. According to Ohm's law, the current passes through the path with the smallest impedance. When eddy current encounters a crack, the path through the crack tip is the shortest and the impedance is minimal for the eddy current flowing through the crack tips. Thus, the eddy current is separated and bypasses the defect via the crack tip, leading to a decrease of the eddy current density at the crack side and an increase at the crack tip. According to Eq. (2), the heating power is proportional to the square of the eddy current density. Thus, a low temperature area is formed on crack sides (blue area in Fig. 1) and a high temperature area is formed at tips (red area in Fig. 1).

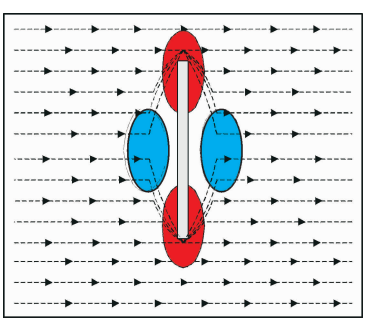

Fig. 1 Eddy current distribution model in crack area

2 Simulation Modeling and Analysis

2.1 Modeling

The numerical studies were conducted using

COMSOL Multiphysics 5.1a, which is based on the Eqs. (2), (3) in the model calculation and analysis. The computing ability of COMSOL can well meet the design simulation of electromagnetic induction heating process, and electromagnetic induction infrared analysis model reflects the coupling phenomena of magnetic field and heat transfer, especially when it applies to electric-magnetic-thermal coupled multiphysics field. The simulation process included two parts: Electromagnetic induction and heat transfer. Modeling analysis was divided into six parts, as shown in Fig. 2.

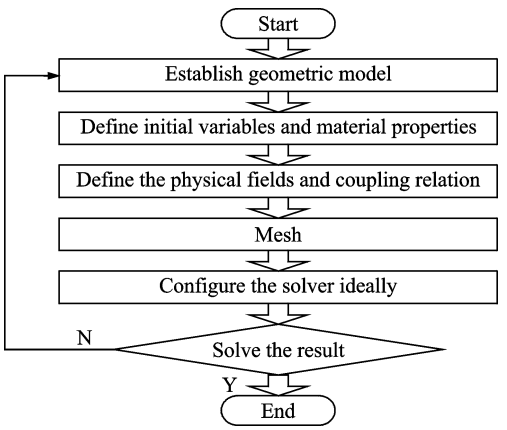

Fig. 2 Simulation modeling

(1) Establish geometric model

The complex model can provide a more accurate simulation while with a higher simulation cost. So a simple geometry instead of a complex one was employed. In order to minimize the model, effective boundary conditions should be used to truncate the geometric model at the proper location to create a shield layer. The model mainly focused on three parts: The coil, the measured object and the shielding layer (air). Each of them was established according to the actual size, as shown in Fig. 3. The size of specimen was set as 240 mm × 50 mm × 5 mm. The fatigue cracks were constructed by narrow rectangular blocks (0.08 mm) with the same width and height but different length, and the lift-off distance between the coil and the steel was 5 mm. Walle studied the effect of crack direction on temperature response[11], and results showed that temperature response would be up to a maximum value when direction of the defect and eddy current were vertical, but when they were parallel to each other, the temperature change was only about 30% of the maximum temperature change. In this case, we placed the crack inside the coil and kept them vertical.

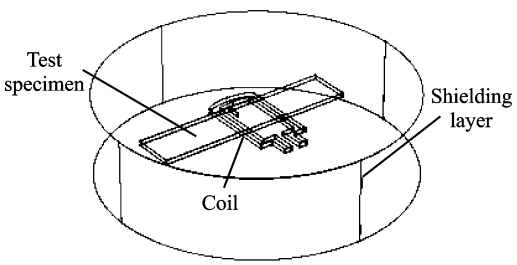

Fig. 3 3D model

(2) Define initial variables and material properties

The initial temperature was set at 20 ℃ for every case of simulation. The coil material was copper, and the test specimen was C45. The dielectric layer between coil and test specimen was air. The specific physical parameters used in the simulation are shown in Table 1.

Table 1 Physical parameters of each part of the model

Material	Density/ ($kg \cdot m^{-3}$)	Thermal conductivity/ ($W/(m \cdot K)^{-1}$)	Electro conductibility/ ($S \cdot m^{-1}$)	Relative permeability	Heat capacity/ ($J \cdot (kg \cdot K)^{-1}$)
Copper	8 700	400	5.9×10^7	1	385
C45	7 750	50.2	$5.0 \times 10^6 6$	400	480
Air	1.2	0.025 7	1.0×10^{-5}	1	1 000

(3) Define the physical fields and coupling relation

A 3D electromagnetic field model was established by using the electro-magnetic-thermal coupling interface in AC/DC module. The magnetic field isolation boundary, the initial value and the type of the exciting current in the coil were determined fist. And then the system were to be coupled with the electromagnetic field and heat transfer field. In this model, the excitation frequency and current were set as 800 kHz and 300 A, respectively, the heat period was 200 ms.

(4) Mesh

The mesh element was chosen to be a free tetrahedron. Considering accuracy and efficiency of the simulation, units with different sizes were used for different parts of the model. The specific parameters are shown in Table 2, and the results of the meshing are shown in Fig. 4 (the air part is not shown).

Table 2 Mesh size of each part of the model

Material	Maximum unit size/mm	Minimum unit size/mm	Maximum unit growth rate	Buckling factor	Resolution of narrow area
Test specimen	8	0.08	1.30	0.2	1.0
Coil	32	4.00	1.45	0.5	0.6
Air	40	7.20	1.50	0.6	0.5

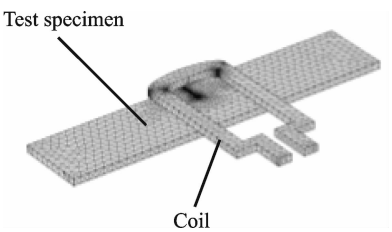

Fig. 4 Mesh generation of geometric model

(5) Configure the solver

In order to analyze the variation of the magnetic field and temperature field with time, a time domain transient linear solver was used. Specifically, the global absolute tolerance was set to 0.001. The time step used backward difference method, the initial step 0.01 ms and the maximum step size 0.1 ms. At the same time, the PARDISO algorithm was adopted to enhance the robustness and fast convergence.

(6) Solve the result

The result of the solver solution was automatically displayed in the Results module of the COMSOL software, and then the result information was viewed as needed. The temperature response on the surface of the steel was recorded and analyzed. Fig. 5 shows the temperature of defect area change curve by Results module.

2.2 Simulation analysis

Depending on the frequency of excitation current, the heating zone can be confined to the surface (surface heating) or to the entire volume of the material (volume heating)[6]. The efficiency

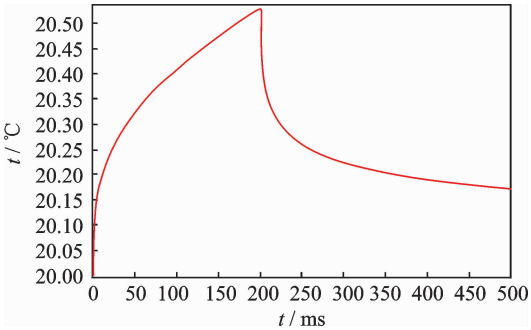

Fig. 5 Temperature change of defect area

of material heating requires optimum frequency for inductive heating and is also affected by electrical properties of the material. If the material is ferromagnetic metals with high permeability, the skin depth will be much small[7]. Therefore, we can neglect the effect of skin depth and consider the heat to be on the surface of the specimens. The solution of surface temperature can be expressed as

$$\Delta T = \frac{2Q}{k}\left(\frac{\alpha t}{\pi}\right)^{1/2} \tag{4}$$

where Q is the heat applied to the surface, α the thermal diffusivity of steel, k the thermal conductivity, and t the time.

A set of fatigue crack models with different lengths were established using COMSOL, and the temperature response change of cracks with $t^{1/2}$ was studied as shown in Fig. 6. Table 3 shows the values of maximum temperature rise and eddy current density of crack tips. It can be seen that the temperature response curve is approximately linearly increased and satisfying Eq. (4). The crack length has a significant effect on the perturbation of the induced current distribution. The longer the crack is, the stronger the obstruction of the induced current is, which leads to obvious heat.

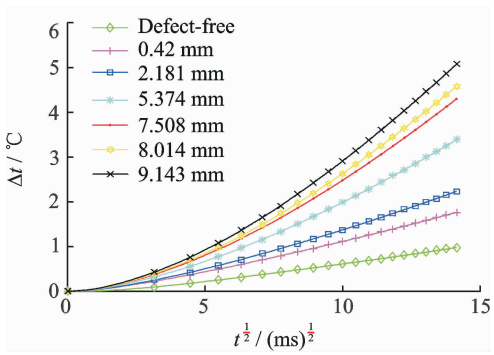

Fig. 6 Numerical temperature responses

Table 3 Maximum temperature rise and eddy current density

No.	Length/mm	Δt/℃	J_s/ (A·m^{-2})
1	0	0.98	$2.249\ 4\times10^7$
2	0.42	1.77	2.4267×10^7
3	1.707	2.24	$2.570\ 3\times10^7$
4	1.987	3.39	$2.610\ 0\times10^7$
5	2.181	4.30	$2.614\ 5\times10^7$
6	3.454	5.07	$2.640\ 4\times10^7$

There is a significant temperature rise in the whole crack area at excitation end time with respect to the excitation start time, when the heating area is only generated around the crack tip, as shown in Fig. 7. For the response at the end of excitation, a square area is selected centered on the midpoint of the crack, and the temperature at a point outside the area is less than the e^{-8} of the center point temperature, which is negligible (The black rectangle is regarded as the crack area in Fig. 7) [12]. Therefore, temperature response in crack area at excitation end time can be chosen as characteristic feature to quantify length.

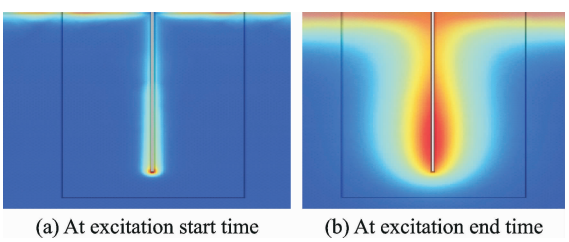

Fig. 7 Temperature rise in the crack area

3 Experiment

3.1 Experiment setup

The system setup of ECPT is illustrated in Fig. 8. A precision induction heating device was used for induction heating, with a maximum excitation power of 2.4 kW, a maximum current of 400 A, and an excitation frequency range of 150—400 kHz. The rectangular coil made of 8 mm high-conductivity hollow copper tube was positioned above the test specimen, with the edge of the coil orthogonal to the defect under inspection, as shown in Fig. 9. The FLIR IR camera was used to record thermal images, which has a resolution of 640 pixel×480 pixel, a thermal sensitivity of 0.035 and a maximum full frame rate of 30 Hz.

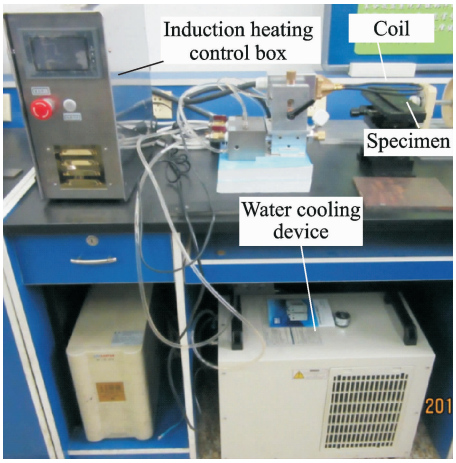

Fig. 8 System setup of ECPT

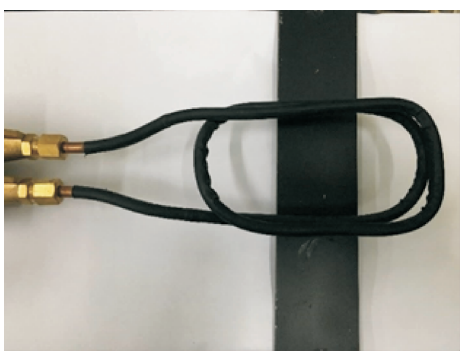

Fig. 9 Excitation coil and specimen

3.2 Test specimen

The raw artificial fatigue crack specimen was the C45 ferritic steel plate, as shown in Fig. 10[13]. The tensile strength and lower yield strength were 620 MPa and 451 MPa, respectively. The middle hole was used to cut notch so as to generate cracks. And four holes arranged on both sides of the middle hole were used to install crack opening displacement gauge. Note that crack length needs to be controlled precisely, and the compliance method was introduced to monitor crack length between 0.4 mm and 9.5 mm.

The wire electrical discharge machining (WEDM) method was used to cut the raw speci-

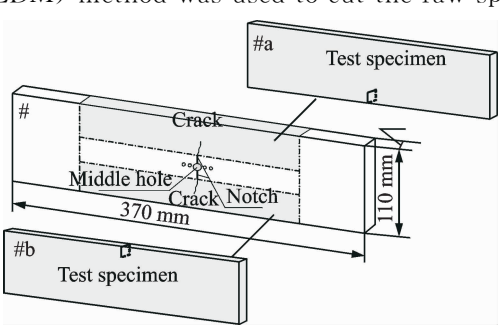

Fig. 10 Fatigue crack Specimen

men according to the dot dash line shown in Fig. 10, and each of them yields two pieces of test specimens (240 mm×50 mm×5 mm).

The crack lengths were measured by optical microscope, and the values of 16 crack lengths were taken as variable, as shown in Table 4. After measurement, the surfaces of test specimens were blackened by flat lacquer, and their emissivity was increased.

Table 4 Crack length

No.	Length /mm	No.	Length /mm
1	0.42	9	6.577
2	1.707	10	7.508
3	1.987	11	7.948
4	2.181	12	8.014
5	3.454	13	8.280
6	3.898	14	9.143
7	5.374	15	9.301
8	5.559	16	9.453

3.3 Experimental analysis

During experiments, both the coil and an IR camera were placed above test specimens (reflection mode). The heating period was 0.2 s and record time was 1 s, which ensured a detectable temperature rise on surfaces of the specimens. Fig. 11 shows the temperature distribution of crack area, where brighter color represents higher temperature. Fig. 12 shows experimental temperature responses. The results are similar to numerical results, which confirms the correctness of characteristic selection.

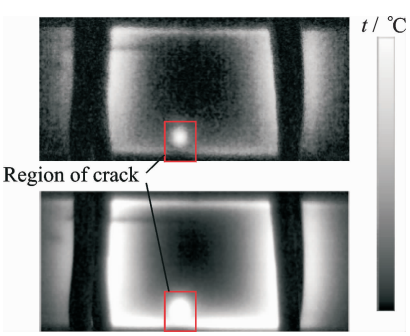

Fig. 11 Temperature contrast of the crack area at the start and the end of excitation

The lift-off distance effect on temperature rise of crack area was studied under three excitation intensity conditions (30%, 60% and 100% of maximum power). As shown in Fig. 13, with the increase of distance, surface temperature rise of specimens first increased and then decreased. It can be seen from the curves, temperature rised to the highest when the lift-off distance is about 15 mm.

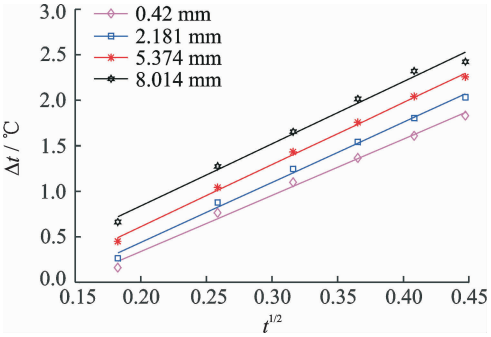

Fig. 12 Experimental temperature responses

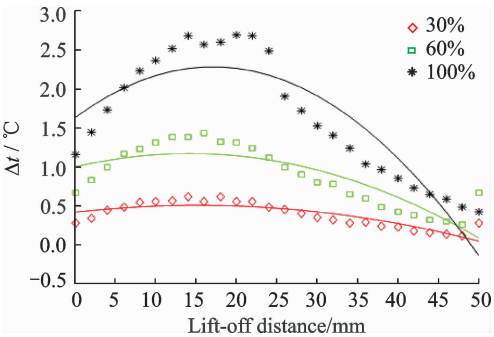

Fig. 13 Relation between lift-off distance and temperature rise

4 Discussions

During the experiment, each crack was tested three times, and three lift-off distances were set at the same time. The mean temperature rise at the excitation end time was extracted from simulation and experiment results, as shown in Fig. 14. The *R*-square of the fitting curves are 0.99, 0.89, 0.90 and 0.91, respectively. The value of the parameter *R*-square represents the fitting effect, and it closer to 1. The fitting is ideal. Clearly, with increasing of the crack length, *L*, there is a good linearity increase in temperature. Both simulated values and experimental values are fitted with crack lengths using the linear formula shown in Eq. (5). This phenomenon can be explained by eddy current distribution model in crack area. The longer the crack length is, the stronger impediment on the eddy current is. Then

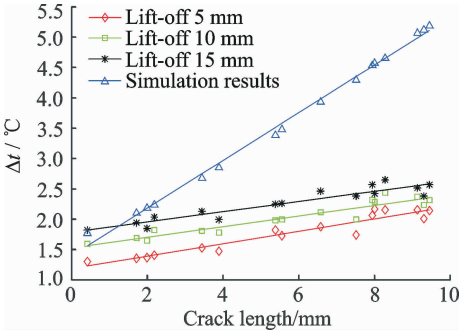

Fig. 14 Relation between the heat and the crack length in the crack area by simulation and test

it causes a higher eddy current density at the crack tips, resulting in a lot of induction heat

$$\Delta T = p_1 L + p_2 \tag{5}$$

5 Conclusions

The relation between a specific temperature response and crack length was studied using ECPT. And a linear relation was verified through numerical and experimental studies. Through multiphysics simulation studies, unique features of temperature distribution were extracted and analysed for the quantification of defect lengths. Experimental measurements showed a good agreement with the simulations. In conclusion, the linear fitted curves between temperature responses and crack lengths can be used as a quantitative evaluation of crack length.

Acknowledgment

This work was supported by the Open Foundation of Key Laboratory of Nondestructive Testing of Ministry of Education of Nanchang Aeronautical University.

References:

[1] HE Yunze, PAN Mengchun, CHEN Dixiang, et al. Eddy current step heating thermography for quantitatively evaluation[J]. Applied Physics Letters, 2013, 103(19): 023112-2698.

[2] WEEKES B, ALMOND D P, CAWLEY P, et al. Eddy-current induced thermography—probability of detection study of small fatigue cracks in steel, titanium and nickel-based superalloy[J]. Ndt & E International, 2012, 49(7):47-56.

[3] DIMAMBRO J, ASHBAUGH D, NELSON C, et al. Sonic infrared (IR) imaging and fluorescent penetrant inspection probability of detection (POD) comparison [J]. Rev Prog Quant Nondestr Eval, 2007, 26: 463-470.

[4] VRANA J, GOLDAMMER M, BAUMANN J, et al. Mechanisms and models for crack detection with induction thermography [J]. American Institute of Physics, 2008(2): 475-482.

[5] WEEKES D B. Investigation of infrared thermography NDE techniques for use in power station environments[D]. London: Imperial College London, Department of Mechanical Engineering, 2011.

[6] BIJU N, GANESAN N, KRSHNAMURTHY C V, et al. Frequency optimization for eddy current thermography [J]. NDT EInt, 2009, 42(5): 415-420.

[7] BIJU N, GANESAN N, KRSHNAMURTHY C V, et al. Simultaneous estimation of electrical and thermal properties of isotropic material from the toneburst eddy current thermography (TBET) time-temperature data [J]. IEEE Trans. Magn, 2011, 47 (9): 2213-2219.

[8] REN W, LIU J, TIAN G Y, et al. Quantitative nondestructive evaluation method for impact damage using eddy current pulsed thermography [J]. Composites Part B Engineering, 2013, 54(1):169-179.

[9] HE Y, PAN M, TIAN G Y, et al. Eddy current pulsed phase thermography for subsurface defect quantitatively evaluation [J]. Applied Physics Letters, 2013, 103(14): 054103-2120.

[10] ABIDIN I Z, TIAN G Y, WILSON J, et al. Quantitative evaluation of angular defects by pulsed eddy current thermography [J]. Ndt & E International, 2010, 43(7):537- 546.

[11] WALLE G, NETZELMANN U. Thermographic crack detection in ferritic steel components using inductive heating[C]// European Conference on NDT. Berlin, Germany: NDT,2006: 25- 29.

[12] FENG Fuzhou, ZHANG Chaosheng, MIN Qingxu, et al. Heating characterristics of metal plate crack in sonic IR imaging[J]. Infrared and laser engineering, 2015, 44(5): 1456-1461. (in Chinese)

[13] OU Yanghui. GB/T 6398—2000 The test method of the fatigue crack propagation rate in metallic materials [S]. Beijing: China Standard Press, 2000. (in Chinese)

Prof. **Feng Fuzhou** received Ph. D. degree in Mechanical Engineering from Tsinghua University, Beijing, China, in 2000. From 2003 to 2004, he studied in the Republic of Korea Kau Ching University as a visiting scholar. From

2005 to present, he has been a full professor in Mechanical Engineering, the Academy of Armored Force Engineering. He mainly engaged in infrared thermography nondestructive detection, fault prediction and health management.

Mr. **Xu Chao** received B. S. degree in Mechanical Engineering from Hebei University of Technology, Tianjin, China, in 2011, and studies at Academy of Armored Force Engineering, Beijing, China, as a master candidate. His research is focused on image processing using eddy current pulse thermography.

Dr. **Zhu Junzhen** studies at Newcastle University, UK, as a Ph. D. candidate. His research is focused on active infrared thermography nondestructive testing and evaluation.

Dr. **Min Qingxu** received B. S. degree in Mechanical Engineering from China University of Petroleum, Qingdao, China, in 2011, and M. S. degree in Academy of Armored Force Engineering, Beijing, China, in 2013. In March 2014, he joined the Department of Mechanical Engineering, Academy of Armored Force Engineering, as a Ph. D. candidate. His research is focused on infrared thermography nondestructive detection, assessment technique and relevant fields.

Mr. **Sun Jiwei** received B. S. degree in Mechanical Engineering from Wuhan University, Wuhan, China, in 2012, and studies at Academy of Armored Force Engineering, Beijing, China as a master candidate. His research is focused on probability of detection using eddy current pulsed thermography.

(Executive Editor: Zhang Bei)